01 Sep 1975

Periodic and Random Excitation of Streamlined Structures by Trailing Edge Flows

W. K. Blake

PERIODIC AND RANDOM EXCITATION OF STREAMLINED STRUCTURES BY TRAILING EDGE FLOWS

William K. Blake
David W. Taylor Naval Ship Research and Development Center
Bethesda, Maryland 20084

ABSTRACT

This paper is an examination of semi-empirical techniques which are shown to be effective in predicting the response of hydrofoils to flow excitation. Examples are given for buffeting by inflow turbulence, excitation by the boundary-layer pressures on the hydrofoil, and linear and non-linear excitation by vortex street formation in the wake. Co-ordinated aerodynamic and hydrodynamic measurements are used in Reynolds number - scaled experiments to determine both the flow induced forces and the hydro-elastic behavior on cantilever struts. An analytical formulation based on normal mode theory is used to combine the results.

INTRODUCTION

The flow excited vibration of hydrofoils and struts is controlled by both the nature of the disturbance in the flow and the bending impedance of the structure. This paper summarizes the results of a series of investigations which were directed at determining the relative importance of various fluid forcing mechanisms on struts at small angle of attack. Characteristics of fluctuating driving forces and of hydrodynamic damping have been measured for a range of strut geometries.

Hydrodynamic fluid loading on a strut is manifested both as added mass and as damping. The inertial loading is flow-independent as long as the entrained mass is small enough and the mean fluid velocity is low enough that the instabilities leading to flutter divergence are unimportant. Velocity-dependent hydrodynamic damping arises from fluid reaction forces which are in phase opposition with the transverse bending velocity. These forces are induced by the potential flow around the strut responding to the small oscillating angle of attack provided by a superposition of the bending velocity and the inflow velocity. Work is done by the strut as it generates vorticity in the wake; Blake and Maga (1975a) provide a characterization of this damping mechanism.

We will consider characteristics of the unsteady excitation forces to depend on the structure of inflow unsteadiness, on the flow in the boundary layer of the strut, and on the properties of the near-wake behind the strut. When the flow leaving the trailing edge does not generate a von Karman vortex street, as is often the case when the edge is sharp, the fluctuating forces are due primarily to the boundary layer turbulence and to buffeting by inflow unsteadiness. These disturbances linearly excite the resonant bending modes of the strut; when the unsteadiness is random in time and space large numbers of modes are excited. In the case of excitation by inflow turbulence an investigation by Mugridge (1970) has characterized the unsteady forces in terms of the spectrum and macro-length scale of the inflow turbulence. The response of the beam to its own boundary layer depends on the magnitudes and the spatial correlation area of the turbulent surface pressures.

When a periodic wake vortex excitation occurs, as is often the case with blunt trailing edges, the pressures are concentrated within a small region of the trailing edge. The speed dependence of the flow-induced vibration of the strut is typically characterized by extra-ordinarily great responses at specific speeds. At speeds for which the frequency of vortex formation coincides with a resonance frequency of the hydrofoil, the vibration levels are dramatically greater than when such a coincidence of frequencies does

not exist. Increases of structural damping in the strut reduce the non-linear coupling of the fluid and structure which brings about that vibration. The problem is not new; the related problem of the flow-excited singing of circular cylinders has occupied the attention of numerous authors. The results of those investigations have provided much theoretical and empirical knowledge of the dynamical constraints on the shedding process. Dimensionless (Strouhal) frequencies for shedding, oscillatory lift coefficients, vortex correlation lengths, and vortex-street drag coefficients have all been well-documented for fixed cylinders. In the case of hydrofoils and struts far less published information exists, and that information is largely theoretical.

In this paper we will first present a brief review of a modal analysis which provides a framework for interpreting measured strut responses. This analysis has been used in assessing the linear excitation due to inflow turbulence and boundary layer pressures. Following this review, new measurements which show the the relationship between the oscillatory pressures at trailing edges and the dynamics of the periodic wakes of rigid, blunt-edged struts will be discussed. We then consider new measurements of the linear and non-linear flow excitations of damped struts by their vortex streets. These struts have geometrically similar cross sections, but varying damping and trailing edge thickness. Finally we will apply the empirical modeling techniques to the non-linear problem of vortex flow excitation

LINEAR RESPONSE TO TURBULENT FLOW EXCITATION

The necessary analytical formulations for fluid-driven struts have been presented by Blake and Maga (1975a) (1975b) We will summarize the analytical treatment in order to form a foundation for the consistent examination of the measured responses of struts to various fluid excitations. The cantilever plate-like strut which is illustrated in Figure 1 is driven by excitation pressures $p_e(\bar{x},\tau)$ and it is loaded by fluid reaction pressures $p_\ell(\bar{x},\tau)$. The quantities $\bar{x} = (x,z)$ and τ are position and time coordinates. The reaction pressures include both inertial and hydrodynamic damping effects; they are differentials between pressures on the upper and lower surface. Excitation pressures on the upper and lower surfaces are

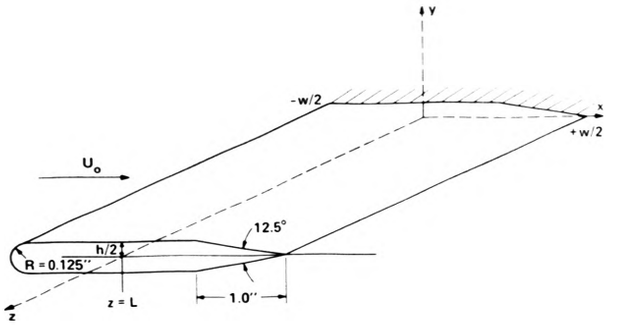

Figure 1 - Co-ordinate System for a Strut Immersed in a Flow Field

correlated in the cases of either buffeting or vortex excitation, and uncorrelated in the case of boundary layer excitation. The transverse vibration velocity is expandable in the normal modes of the strut

$$v(\bar{x},\tau) = \Sigma\, v_{mn}(\tau)\, \Psi_{mn}(\bar{x})$$

where

$$\int_{A_s} \Psi^2_{mn}(\bar{x})\, d\bar{x} = A_s$$

is the area (Lw) of the strut. The plate motion is then expressed as

$$\ddot{v}_{mn}(\tau) + \beta\dot{v}_{mn}(\tau)+\omega^2_{mn}v_{mn}(\tau)=(m_p)^{-1}[\dot{p}_{e_{mn}}(\tau)-\dot{p}_{\ell_{mn}}(\tau)] \quad (1)$$

where β is a material damping coefficient, ω_{mn} is the in-vacuo resonance frequency of the m,n mode, and m_p is the area density of the plate. The modal excitation pressure is

$$p_{e_{mn}}(\tau) = \frac{1}{A_s}\int_{A_s} p_e(\bar{x},\tau)\, \Psi_{mn}(\bar{x})\, d\bar{x}$$

and similarly for $p_{\ell_{mn}}(\tau)$ which depends on $v_{mn}(\tau)$. The modal excitation pressure is considered to be a random variable and independent of $v_{mn}(\tau)$ for linear turbulence excitation, but in cases involving vortex shedding it may depend on the bending velocity and it may not be stochastic. For any <u>linear</u> turbulence excitation the spectral density of transverse acceleration at a point $\bar{x}_o$, $\phi_A(\bar{x}_o,\omega)$, has been shown in Reference 5, to be given by a summation over resonant bending modes;

$$\frac{\phi_A(\bar{x}_o,\omega)m_s^2}{q^2} = \Sigma_{m,n} \frac{\Psi_{mn}(\bar{x}_o)}{[(\frac{\omega_{mn}}{\omega})^2-1]^2+(\frac{\omega_{mn}}{\omega})^2\,\eta_T^2} \quad (2)$$

$$\int_{A_s}\int_{A_s} \frac{\phi_p(\bar{x}_1,\bar{x}_2,\omega)}{q^2}\ \Psi_{mn}(\bar{x}_1)\ \Psi_{mn}(\bar{x}_2)\ d(\frac{\bar{x}_1}{A_s})\ d(\frac{\bar{x}_2}{A_s}),$$

where $\bar{x}_1$, and $\bar{x}_2$ are locations in the plane of the strut. In this expression $q=\rho U_\infty^2/2$ where ρ is the fluid density, U_∞ is the mean velocity, m_s is the wetted mass per unit area of the strut, and η_T is the total loss factor of the m,n mode; it includes both hydrodynamic and hysteretic damping. The resonance frequency now applies to the cantilever plate in water. The cross-spectral density of the pressure on the strut, $\phi_p(\bar{x}_1\bar{y}_2\omega)$, has a particular form depending on the type of excitation. The integral in equation (2) expresses the spatial matching of the chordwise (x) and spanwise (z) correlation length scales typical of the fluid pressure say (λ_x,λ_z), with the characteristic wavelengths of bending motion, say $(\lambda_{p_x},\lambda_{p_z})$. In Reference 6 it was assumed that the correlation area of the fluid pressure satisfied the inequality $(\lambda_x\lambda_z) << (\lambda_{p_x}\lambda_{p_z})$ for both boundary-layer and inflow-turbulence excitation. The cases of both linear and non-linear vortex-excitation will be treated subsequently. In any of these cases the integral is considered as a mean-square modal force (or oscillatory lift) coefficient, for the flow-excited strut.

Equation (2) has been evaluated in Reference 6 for comparison to the measured acceleration levels of specific modes of a 2.75 x 20 x 0.25 inch thick stainless steel cantilever strut in flowing water. The strut had the same section shape with a sharp trailing edge as shown in Figure 1. Measurements* were obtained for the uniform beam modes (1,0), (2,0), (3,0), and (4,0) illustrated in Table I. The experimental and

TABLE I

RESONANCE FREQUENCIES (Hz) OF BEAMS** IN WATER

Shape	Order	Brass, L=18"	Steel L=18 7/16"
	1,0	70	115
	0,1	170	260
	2,0	186	298
	3,0	375	580
	1,1	520	850
	4,0	630	987
	2,1	870	
	5,0	940	

theoretical evaluation of the acceleration was made only at frequencies corresponding to $\omega = \omega_{m,o}$. The integral in equation (2) was evaluated for boundary layer excitation using measured cross-spectral densities in a wind tunnel on a two-dimensional, Reynolds number-scaled version of the strut and the measured mode shapes $\Psi_{m,o}(\bar{x})$. Buffeting response was estimated by using the measured free-stream turbulence spectra in the water tunnel and Mugridge's (1970) theoretical oscillatory lift coefficient. Figure 2 shows the

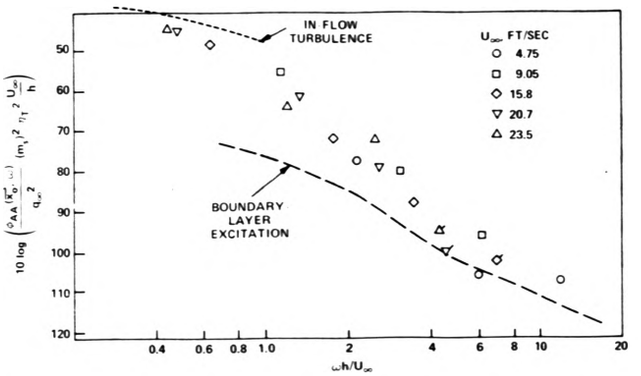

Figure 2 - Comparison of Theoretical and Measured Modal Acceleration Spectra for a Stainless Steel Strut. Taken from Blake and Maga (1975b)

measured dimensionless acceleration spectral density with frequency normalized as $\omega h/U_\infty$. The dimensionless acceleration spectral density is seen to be compatible with equation (2) when $\omega = \omega_{m,o}$. Theoretically calculated levels of the integral in equation (2) are shown as dotted lines. Boundary layer excitation accounts for the high frequency acceleration while buffeting by inflow turbulence (which has a root-mean-square level of 2% of U_∞) causes low frequency acceleration. The boundary layer excitation for $\omega h/U_\infty > 2$ is dominated by the pressure fluctuations exerted in the downstream portion of the strut surface. These pressures are highest due to the adverse static pressure gradient existing there. At lower frequencies, the calculated boundary layer excitation is controlled by a large-scale eddy structure which is generated at the circular leading edge of the strut. Separation of the laminar boundary layer at the leading edge generated this unsteadiness. The aerodynamic measurements disclosed that the large-scale pressure field induced by the separation increased as the angle of attack increased. The higher frequency boundary layer pressures were unaffected by the small angle of attack. The theoretical model for the calculated buffeting response is valid for $\omega h/U_\infty < 1$. For $1 < \omega h/U_\infty < 3$ it is difficult to distinguish physically between the effects of in-flow turbulence and the effects of separation because both disturbances are

* A full description of the procedure and instrumentation is given by Blake and Maga (1973) and it is summarized in References 5 and 6.

**w = 2.5 inch, t = 0.072 inch

of the same spatial scale, and both are convected at speeds near U_∞. This result is typical of those which were obtained on a series of beams with varying chord and length. It is to be noted that values of the total loss factors for each mode were required in the normalization of Figure 2. For the strut of this example the loss factors were dominated by speed-dependent hydrodynamic damping throughout most of the speed range. This loss mechanism will be further examined in section 4. The kinematic basis for scaling the aerodynamic pressures to calculate the hydrodynamically-induced bending response was provided by wake measurements. In experiments in both media mean velocity profiles and turbulence intensity spectra were obtained at corresponding locations in the wakes just downstream of the trailing edges.

CHARACTERISTICS OF THE OSCILLATORY LOADING ON STRUTS WITH FIXED EDGES

The remainder of the paper is concerned with the excitation of the struts by periodic vortex streets. The struts have the same basic section shape as that diagrammed in Figure 1, but in these cases the trailing edge was blunted (slightly reducing the chord from 2.75 inches to 2.5 inches) as shown in Figure 3.

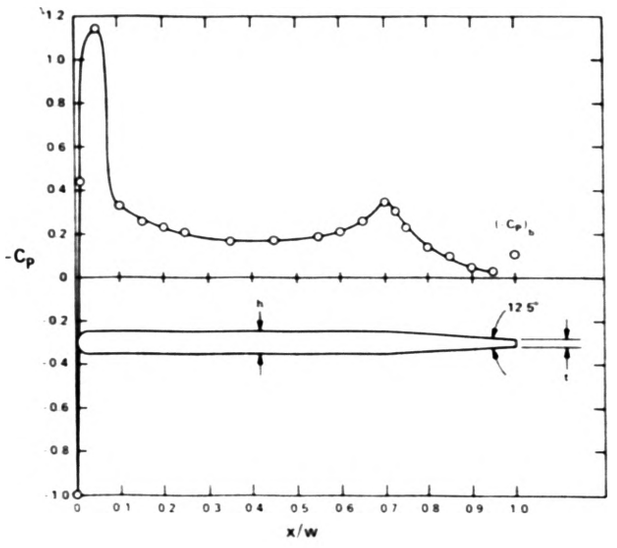

Figure 3 - Cross-Section Shape and Pressure Distribution of the Strut with t/w=0.0266, h/w= 0.091 at Zero Angle of Attack

As in References 5 and 6 the fluid excitation forces were determined aerodynamically and the flow-induced bending response was determined in a water tunnel. The procedures were the same as those in References 5 and 6. These results are new and will be considered in more detail than in the last section. Although two trailing edge thicknesses were used in the water tunnel experiments, t = 0.036 inch (t/w = 0.0133) and t = 0.072 inch (t/w=0.0266), only the scaled-up version of the larger thickness edge was examined in air. The aerodynamic measurements of the wake structure as well as of the chordwise dependence of the oscillating pressure were made on a two-dimensional rigid strut with w = 21 inches; hydrodynamic measurements of the flow-excited acceleration were made on damped cantilever struts with a chord of w = 2.5 inches. The air measurements on the rigid strut are expected to apply to the linear flow excitation of struts.

This section is concerned with the results of the measurements in air which were performed in the David W. Taylor Naval Ship Research and Development Center (DTNSRDC) Anechoic Flow Facility (AFF). The static pressure distribution for the strut is shown in Figure 3. Over most of the chord and except for x/w > 0.8 it is identical to that given previously in Reference 6. The pressure coefficient is defined as $(P-P_\infty)/q$ where P and P_∞ are the static pressures on and far from the strut respectively. The base pressure coefficient is designated as $(C_p)_b$. The boundary layer development on the strut is the same as that described in Reference 6.

The frequency spectra of fluctuating pressures at the trailing edge of the strut with t/w = 0.0266 were dominated by a tone at frequencies $f_s = \omega_s/2\pi$ which satisfy a Strouhal number which is most conveniently defined as

$$N_{st} = f_s t/U_\infty = 0.148.$$

(This frequency may be put in the perspective of the last section and Figure 2 by noting that it corresponds to a dimensionless frequency, $\omega_s h/U_\infty = 3.6$). This form of nondimensionalization for the frequency is not universal, see Bearman (1967) and Blake (1975), but it is a constant for the air and the water experiments considered here. The wake structure behind the rigid strut at the Reynolds number $U_\infty t/\nu = 2.92 \times 10^4$ (U_∞ = 100 ft/sec, t = 0.56 inch) is shown in Figure 4. The method of data acquisition is described by Blake (1975). The cross-stream variation of the periodic velocity fluctuations, $u'(f_s)/U_\infty$, measured in a 7% frequency band centered on $f = f_s$, is seen to have local maxima, $u'(f_s)_m/U_\infty$, at distances y_o apart. This wake dimension first decreases then increases with increasing distance downstream of the edge while the local maxima in the

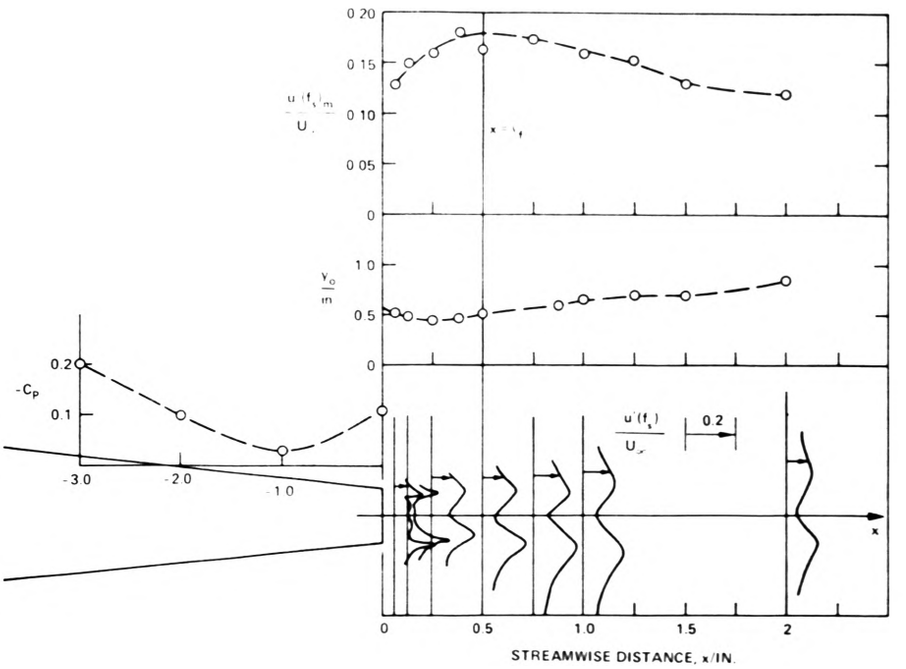

Figure 4 - Composite Diagram of Near-Wake Dynamical Properties Showing Filtered Wake Intensity, $u'(f_s)/U_\infty$, Width Parameter, y_o, and Static Pressure Coefficient Distribution, $(-C_p)$. Note that the Streamwise Co-ordinate Scale has been Expanded for $x > 0$.

wake intensity display an absolute maximum near the point of minimum y_o. This point has been defined by Bearman (1965) as the end of the formation region of the vortex which occurs a distance $x = \ell_f$ downstream of the edge. The spatial growth of the disturbances shown in Figure 4 is demonstrative of the instabilities which occur in free shear layers; the observed formation length, $\ell_f = 0.9t$, is comparable to that observed by Bearman (1965) and Blake (1975) for trailing edges without splitter plates.

A narrowband, 3 Hz bandwidth, spectral analysis of the fluctuating pressures at the trailing edge showed the dominant periodic component to be superimposed on the boundary layer pressure that would have existed if the edge had been sharp. However, as we shall presently see, the periodic component of pressure dominated the excitation of the strut. The narrowband, mean-square levels of periodic pressure on the surface of the rigid strut at the trailing edge are shown normalized on the free-stream dynamic head, in Figure 5. The bandwidth of analysis was greater than that of the pressure fluctuations at speeds below $U_\infty = 100$ ft/sec. Frequency has been made dimensionless as a Reynolds number

$$N_{R_e} = \frac{ft^2}{N_{st}\nu} = \frac{U_\infty t}{\nu}$$

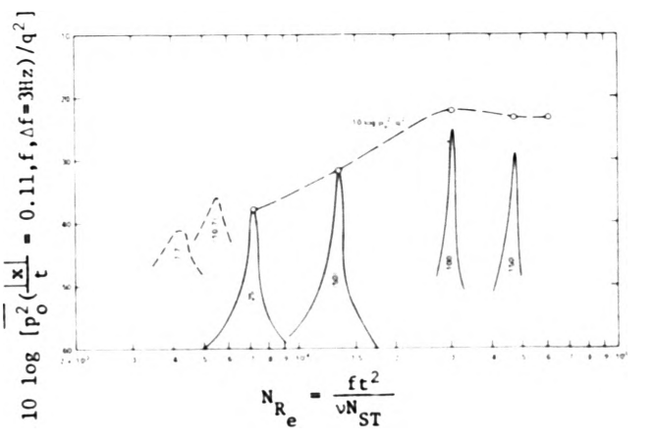

Figure 5 - Mean-Square Fluctuating Pressure on Rigid Strut at $|x|/t=0.11$ ($x/\ell_f=0.13$) and $t/c=0.0266$ Shown as a Function of Trailing Edge Reynolds Number. Measured Directly in Air (_____); Indirectly Determined from Wake Survey of Vibrating Beam (— —); Total Mean-Square Values (---). Values of U_∞/ft/sec Pertaining to the Data are shown in Parenthesis.

where ν is the kinematic viscosity of the fluid. The pressure was measured at a distance $|x|/t = 0.11$ upstream of the trailing edge. The locus of levels described by the dotted line, $\overline{p_o^2}(f_s)/q^2$, are the total mean square pressure levels which reach a maximum value at a frequency $f\,t^2/N_{st}\nu = 31700$. For lower Reynolds numbers, the level of oscillating pressure appears to

increase roughly as the square of Reynolds number. The dotted spectra were deduced from the water-tunnel wake survey using a method which will be described later in this paper. The measured chordwise distribution of fluctuating pressure showed maximum levels at the trailing edge. For this strut the experimentally-determined chordwise pressure distribution can be expressed for our convenience by the equation

$$\overline{p^2}(|x|/t,f_s)/q^2 = \overline{p_0^2}\,(|x|/\ell_f=0.3,f_s)/q^2[10|x|/t]^{-1} \qquad (3)$$

which is valid for $0.11 < x/t < 20$. Here $\overline{p_0^2}$ is the mean square pressure evaluated at $x = 0.3\,\ell_f$. A more universal form of equation (3) in which t is replaced by ℓ_f was shown by Blake (1975) to apply for different edge shapes. The chordwise pressure distribution is deterministic, while the spanwise spatial variation is random. At this point it is worth noting that the magnitude of the base pressure coefficient, $-C_{p_b}=0.11$ (see Figures 3 and 4), of the current experiment, is somewhat larger than that measured for larger trailing edge thicknesses. Although we are gaining some experience in relating the fluctuating pressure levels with mean-flow parameters, a complete set of data which gives the behavior of p_0^2/q^2 for various base pressure coefficients is not yet available. However, as shown in Figure 6 there appears to be a relationship

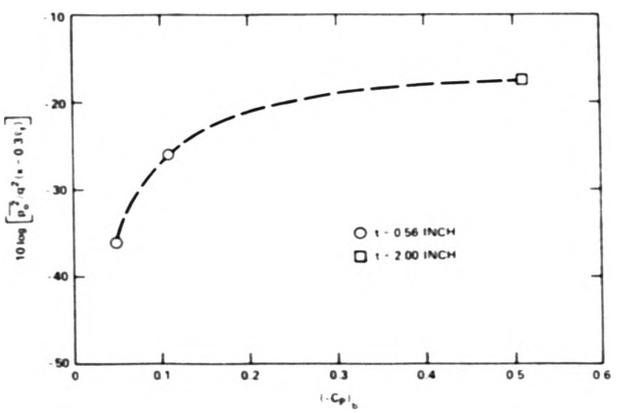

Figure 6 - Variation of Mean-Square Pressure, on Blunt Edged Struts at $x = 0.3\,\ell_f$, with Static Base Pressure Coefficient

between the base pressure coefficient and fluctuating pressure, at least for the blunt edges examined so far.

The fluctuating pressure at the edge of the strut has been related to the strength and structure of the wake vorticity by Blake (1975) through an empirical function

$$\left(\overline{p_0^2}(x/\ell_f=0.3,f_s)\right)^{1/2}/q = 2\,\frac{U_s}{U_\infty}\,\frac{\kappa}{U_\infty \ell_f} \qquad (4)$$

where U_s is the mean velocity at the separation points which is defined as

$$U_s/U_\infty = \sqrt{1-C_{p_b}}\,.$$

The root-mean-square vortex strength κ is given by

$$\kappa = u'(f_s)_m\, r_o \qquad (5)$$

where $u'(f_s)_m$ is given in Figure 4 and $r_o = y_o/4$. This definition is predicated on the assumption that the vortex cores of the upper and lower vortex rows occupy the cross-wake regions $0 < y < y_o/2$ and $-y_o/2 < y < 0$ respectively. A similar assumption has been made by both Schaefer and Eskinazi (1959) and Fage and Johanson (1927). The local maxima in the velocity fluctuations are therefore interpreted as the peripheral velocities at the extremities of the vortex cores. Equations (4) and (5) give a means of estimating the level of fluctuating pressures given the measured intensity distributions of the velocity fluctuations in the wake of a strut.

MEASURED HYDRO-ELASTIC MOTIONS OF CANTILEVER STRUTS

The second, hydrodynamic, phase of the characterization of singing and non-singing hydrofoils has been conducted in an open-jet water tunnel on cantilever struts which were nominally 18 inches in length and protruded into the flow from a 200 lb. block of stainless steel. In this investigation all the struts had nearly the same chord but they had varying degrees of mechanical damping which was incorporated by using constrained-layer constructions. For most damping treatments the base structure, element 1 in Figure 7, was 0.191 inch thick, the visco-elastic damping layer was .021 inch thick, and the constraining layer was 0.035 inch thick. The nominal overall thickness of the struts was h = 0.25 inch. By constructing the base and constraining portions of the struts with combinations of brass and steel, the damping of the composite could be varied. The visco-elastic material was the same for all damped struts with one exception. That strut was damped with a layer of damping tape, Scotch Brand (3M) #428A UAX R 5182. Figure 7 shows the measured loss factors, η_s, of the cantilever struts

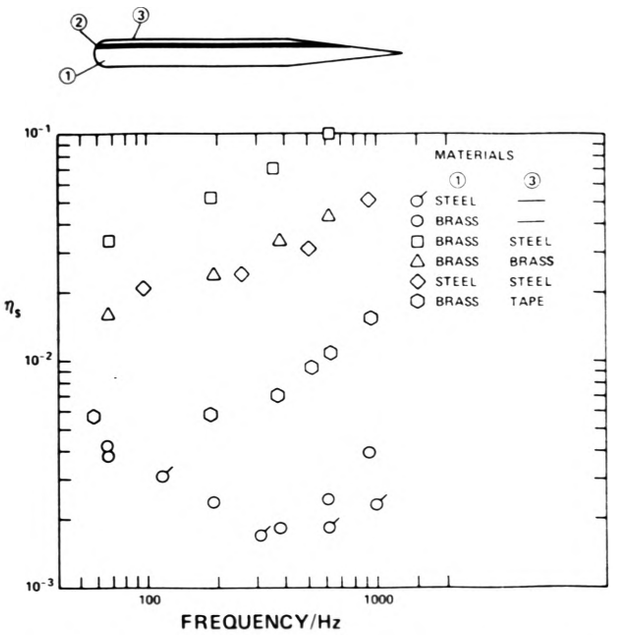

Figure 7 - Total Loss Factors for All Cantilever Struts used in the Study. Measurements were Obtained at U_∞=0 using Reverberation Times of Structural Vibration Following an Impact

in still water for most of the beams considered in the experimental program. The damping in the plain brass and steel struts was controlled by dissipation in the clamp and losses in the composite struts was controlled by the viscoelastic layer. The high loss factors for the brass-steel strut are made possible by the high modulus of the steel constraining layer compared to that of the brass base plate. It is noteworthy that the measured loss factors of the cantilever struts agreed with calculated values obtained with the theory of Ross et al. (1959) for sandwich constructions to within 20%.

The strut vibration was characterized by both simple beam and torsion modes as demonstrated by the mode shapes and resonance frequencies in Table I. The mean-square acceleration, $\overline{a^2}$, of the strut was measured near the mid-chord and so that the torsion response could not be examined in detail. Also, the loss factors were obtained following an impact which was applied also near the mid-chord so that only the simple beam modes could be examined. Figure 8 shows the frequency dependence of the flow-excited mean-square, narrowband, acceleration measured in a 2.5 Hz frequency bandwidth for the stainless steel strut with t = 0.072 inch. The responses of two bending modes and the forced non-resonant response at f = f_s are all shown, the torsion mode response is suppressed. The acceleration has been made dimensionless using the total wetted mass per unit area of the strut, m_s, and the

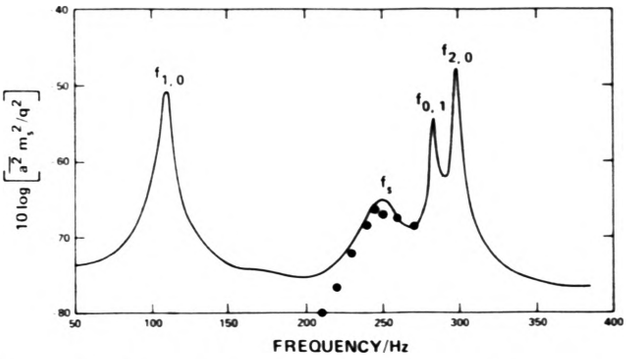

Figure 8 - Dimensionless Acceleration in 2.5 Hz Bands of Steel Strut with t=0.072" at U_∞=10.4 ft/sec Showing both Resonant Mode Response and Forced Vibration at f=f_s. Points (...) are Calculated using Data of Figure 5 and equations (6) and (8).

dynamic pressure q. By comparing the spectra of Figures 2 and 8, we can account for the relative importance of the three fundamental excitation mechanisms. We first recall that $2\pi f_s h/U_\infty$ = 3.6; this dimensionless frequency corresponds to the lower frequency limit of turbulent boundary layer excitation in Figure 2. Thus the (2,0) mode of the strut is driven by this mechanism. On the other hand the (1,0) mode, which occurs at a frequency $f_{1,0}h/U_\infty$ = 1.4, is excited by a combination of sources which involve in-flow buffeting and convected eddies generated by leading edge separation.

From spectra such as this, acceleration levels for each mode were determined as a function of speed. Figure 9 shows the speed dependence of the acceleration of each of the modes (1,0), (2,0), and (3,0) of undamped stainless steel struts. The open points in the figure pertain to measured non-singing resonant responses which were determined with t = 0, and w = 2.75 inches as described in Section 2. The closed points are for t = 0.072 inch and the extraordinarily high values of acceleration occur at those speeds for which $f_s = f_{n,o}$; the levels are in excess of 50 decibels greater than the vibration levels with the sharp edge. The speed dependence of the flow-induced acceleration of the steel-steel damped strut is shown in Figure 10. In this case, the acceleration levels are considerably less amplified at coincidence speeds compared to the cases of the lightly damped strut. In the highly-damped cases, the flow excitation caused by vortex shedding was very nearly linear in the sense of Section 2 even when $f_{n,o} = f_s$. This was established by calculating the ratios of the measured responses of each singing strut to that of the same, non-singing strut with vanishing trailing edge thickness. The frequency and speed dependence for these ratios closely resembles the spectra in Figure 5. Since the

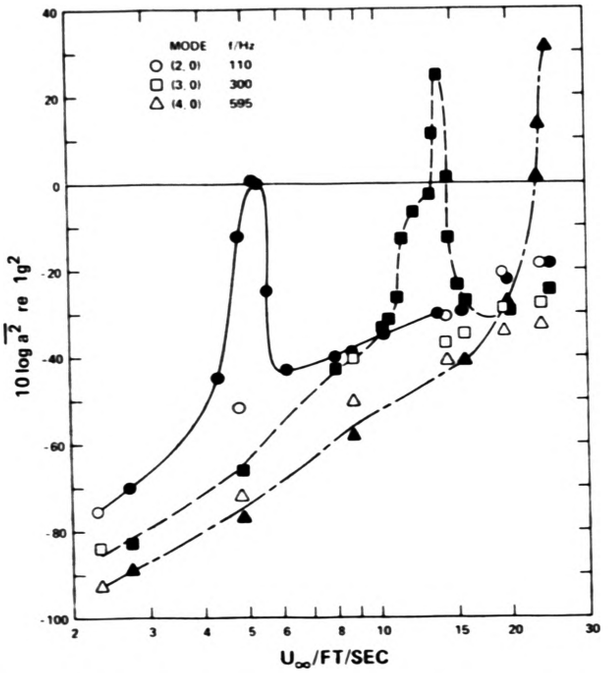

Figure 9 - Flow-Induced Acceleration from Bending Modes of Stainless Steel Cantilever Struts with Sharp (open points) and Blunt (closed points) Trailing edges. Blunt Edges have Thickness, t=0.072 inch, the Frequency Bandwidth of Analysis is 5 Hz.

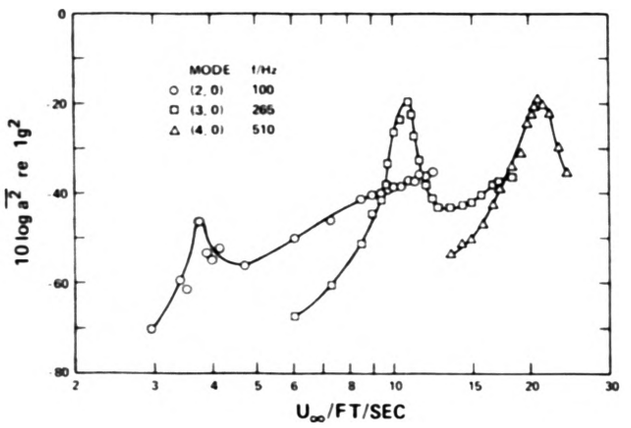

Figure 10 - Speed Dependence of Flow-Induced Acceleration of Steel-Steel Damped Cantilever Strut with Blunt Trailing Edge. The Edge has Thickness t=0.072 inch, the Frequency Bandwidth of Analysis is 5 Hz.

non-singing, linearly-excited strut motion increases uniformly nearly as U_∞^4, these ratios of singing to non-singing acceleration provided a qualitative measure of the lift coefficient.

Total loss factors for the singing struts, η_T, determined as functions of speed, showed anamalous behavior at speeds for which $f_s = f_{n,o}$. As an example, we examine the data for the (2,0) mode of the stainless steel struts in Figure 11. While the beam was

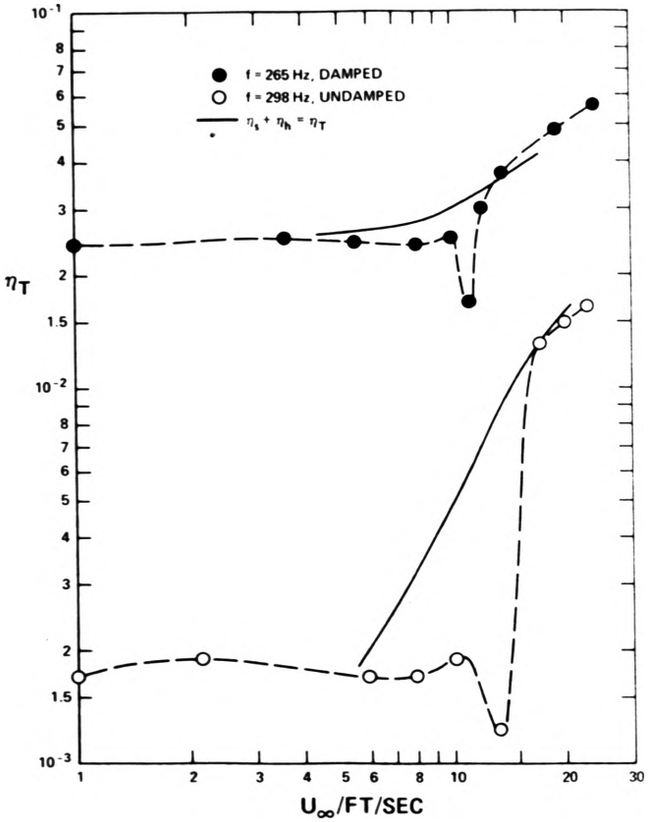

Figure 11 - Loss Factors for Damped and Undamped Steel Struts Vibrating in (2,0) Mode for both Blunt and Sharp Trailing Edges.

flow-excited an impact was remotely applied to the strut and the reverberation time of the resulting vibration was measured. Reductions in the apparent damping occurred whenever $f_s = f_{n,o}$. It appears that in the mechanism of self-excitation, the coupling of the structural motion with the vortex formation is such as to completely overcome whatever hydrodynamic damping that would have existed if the trailing edge had been sharp. This is seen by comparing the measured loss factors with the values of hydrodynamic damping which are calculated using relationships in reference 5. The total damping coefficient is assumed to be a superposition of structural, η_s, and hydrodynamic, η_h, effects. Structural damping, shown in Figure 7, is assumed to dominate at $U_\infty \simeq 0$ and hydrodynamic self-excitation effects dominate for $U_\infty > 5$ ft/sec. In the case of the steel-steel strut, self-excitation effects on the observed damping were much less pronounced and they were most noticable in the immediate region of $f_s = f_{n,o}$. We also note that frequency lock-in was observed to occur near $f_s = f_{n,o}$, the range of speeds for which both the amplitudes were high and the loss factors were low. The root-mean-square displacement amplitudes of motion were

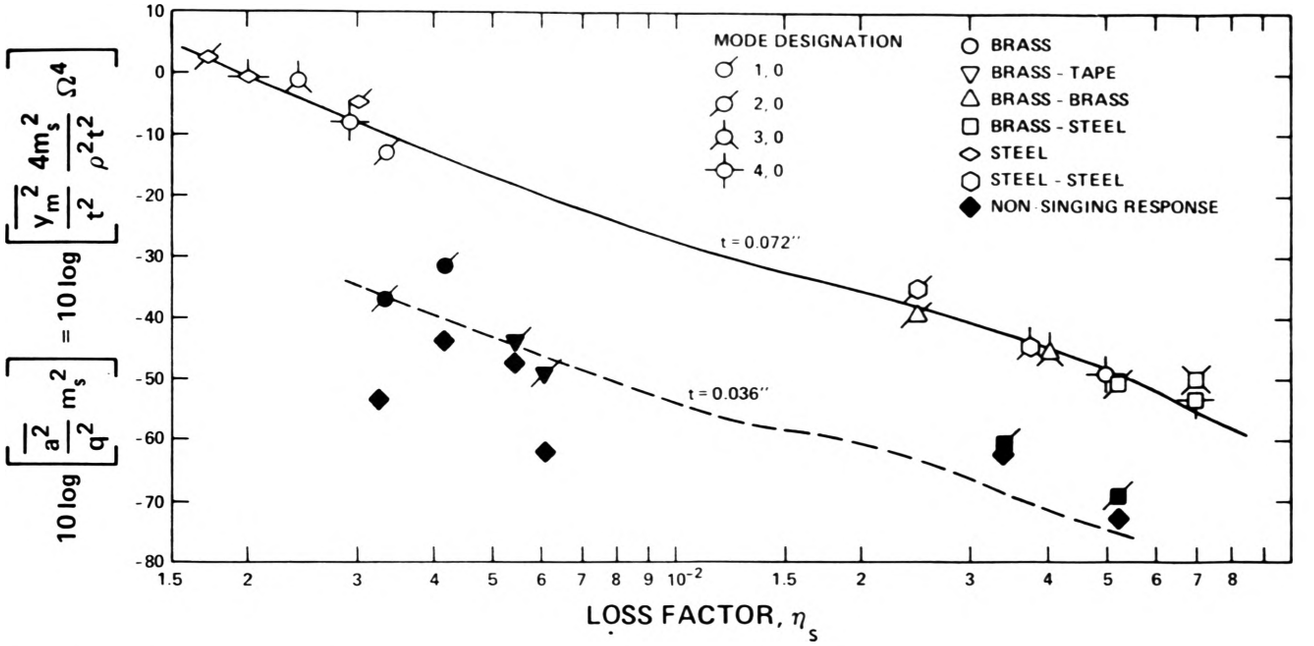

Figure 12 - Dimensionless Modal Acceleration Levels, in 5 Hz Bands, Shown as a Function of Loss Factor. Data is shown for t=0.036 in ch and t=0.072 inch for All Struts Tested. Lines (——) and (- -) are Calculated Results for Non-Linear Oscillator.

less than 10^{-2} t for all modes of all the struts.

The maximum modal acceleration levels for the various bending modes of the different struts are summarized as functions of damping and dynamic head in Figure 12. The loss factors are those measured in water at U_∞=0. The normalization of this figure permits the acceleration levels to be interpreted in an alternative fashion which expresses the modal amplitude, $y_m^2 = \omega_m^4 a^2$, as a fraction of trailing edge thickness t. In this alternative representation we have let

$$\Omega = 2\pi N_{st}.$$

For the t = 0.072 inch edge the tight collapse of the dimensionless acceleration indicates that the hydro-elastic coupling is affected more by the damping than by the order of the mode. The acceleration appears to decrease as η_s^{-4} for light damping in the beams and as η_s^{-2} as the damping is increased above $\eta_s = 3 \times 10^{-2}$. Additional data is shown for the t = 0.036 inch edge. For this edge there is more scatter, the beam did not sing as strongly as it did for t = 0.072 inch and the flow excitation was not more than 20 decibels greater than the non-singing, sharp-edged response. This data does show a dependence on loss factor in good agreement with that of the thicker edge. For $\eta_s > 3 \times 10^{-2}$ vortex-induced response cannot be distinguished from the non-singing motion of the sharp-edges strut.

MATHEMATICAL MODELS OF HYDRO-ELASTIC BEHAVIOR

The theoretical model for the linearly excited acceleration of the cantilever strut, equation (2), can be modified slightly to express the mean square acceleration levels in narrow bands, Δf. In terms of the dynamic head and m_s we have

$$\frac{\overline{a^2(\bar{x}_o,f)}m_s^2}{q^2} = \frac{\overline{\Psi_{m,o}^2(\bar{x}_o)}\overline{C_{L_o}^2(f)}}{\left[1 - \left(\frac{f_{m,o}}{f}\right)^2\right]^2 + \eta_1^2\left(\frac{f_{m,o}}{f}\right)^2}. \quad (6)$$

The integral in equation has been represented as an oscillatory lift coefficient spectrum, $C_{L_o}^2(f)$, which may be expressed in terms of a pressure spectrum and correlation lengths in the following manner.

Measurements of the statistical nature of the pressures at blunt trailing edges, Blake (1975), suggest that the cross-spectral density can be approximated, using equation (3), as

$$\Phi(\bar{x}_1,\bar{x}_2,\omega) = \overline{p_o^2}\left[\left(\frac{10|x_1|}{t}\right)\left(\frac{10|x_2|}{t}\right)\right]^{-1/2}\Phi(\omega)\, R_p(z_1 - z_2) \quad (7)$$

where $\Phi(\omega)$ is the auto-spectral density of the pressure at any point. $R(z_1 - z_2)$ is the spanwise correlation function of the pressure, and $p_o^2 = p_o^2$ ($x = 0.3\, \ell_f, f_s$). Assuming that the spanwise correlation length,

$$\ell_c = \int_o^\infty R_p(z)\, dz,$$

is much less than the bending wavelength, equation (7) allows the integral of equation (2) to be approximated as

$$\overline{C_{L_o}^2}(f) = \overline{p_o^2} \cdot G(f) \left(\frac{4t}{w}\right)^2 \left(\frac{2\ell_c}{L}\right) \left(\frac{L_w}{L}\right) \qquad (8)$$

where $G(f)\Delta f \equiv 2\Phi(\omega)\Delta\omega$. The term $(\frac{4t}{w})$ expresses an average of the deterministic chordwise pressure distribution over chord, w; it is an average over w of equation (3). The term L_w/L is the fraction of the total length of the strut over which the fluid is flowing. In the experimental configuration, the strut protruded into the open jet of a water tunnel so that $L_w/L < 1$. The spectrum $C_{L_o}^2(f)$ is considered to hold for those situations in which the hydrofoil motion is small enough to have no influence on the shedding mechanism. A wake survey similar to that of Figure 4 was conducted behind the steel undamped hydrofoil with t = 0.072 inch in the water tunnel* at speeds for which very strong singing did not occur. These surveys yielded velocity spectral densities, $G_u(f)$ and wake thickness parameters, y_o for implementation in equations (4) and (5) in order to calculate $\overline{p_o^2}\, G(f)$ according to

$$\frac{\overline{p_o^2}\, G(f)}{q^2} = 4\left(\frac{U_s}{U_\infty}\right)^2 \frac{G_u(f) r_o^2}{U_\infty^2 \ell_f^2} .$$

The resulting pressure spectra for U_∞ = 7.7 ft/sec and U_∞ = 10.7 ft/sec are shown in Figure 5. These spectra are in excellent agreement with those obtained in the wind tunnel experiment on the geometrically similar larger strut.

The evaluation of equation (6) was made for U_∞ = 10.4 ft/sec in the case of non-resonant motion of the (2,0) bending mode of the beam. The motion of the (0,1) torsion mode was ignored because the accelerometer was not positioned to measure this mode. Equation (6) was evaluated using ℓ_c = 4t from Blake (1975) and L_w/L = 0.7 from the experiment configuration. The computation, which is shown as the heavily dotted line in Figure 8, agrees well with the measured acceleration. It substantiates the hypothesis of linear flow excitation of the beam and it provides a basis for our analysis of the non-linear hydroelastic behavior.

We turn now to the non-linear hydro-elastic coupling that can control the response to periodic vortex streets. Unfortunately no fully satisfactory analysis exists which correctly portrays the characteristics of the hydroelastic coupling. Recently Hartlen and Currie (1970) suggested an analytical description of the fluid-structure coupling as satisfying the non-linear Rayleigh equation. Later Skop and Griffin (1973) and Griffin, Skop, and Koopman (1973) modified the model and extended comparisons of the model with existing data. The fluid oscillator model of Hartlen and Currie (1970) will be applied to the struts of the current study. The lift coefficient is postulated as satisfying

$$C_L'' - \alpha\left(\frac{\omega_s}{\omega_h}\right) C_L' + \frac{\gamma}{(\omega_s/\omega_n)} (C_L')^3 + \left(\frac{\omega_s}{\omega_n}\right)^2 C_L = bY_n' \qquad (9)$$

where $C_L = C_L(\omega_n\tau)$ and $C_L' = \frac{dC_L(\omega_n\tau)}{d(\omega_n\tau)}$. Here, again, τ is time, $\omega_n = 2\pi f_n$ is the resonance frequency of the strut, and $Y_n = y_n(\omega)/t$ is the normalized modal displacement, $v_n(\omega) = \dot{y}_n(\tau)$. The coefficients α and γ are assumed to be characteristic of the vortex generation process; b is a coupling parameter. For rigid struts $Y_n' = 0$ so that solution to equation (9) is

$$C_L = C_{L_o} \cos 2\pi f_s \tau$$

where C_L is the square root of the oscillatory lift coefficient spectrum on a rigid strut, i.e. with $y_n = 0$, given by equation (8). It is related to the parameters of equation (9) by

$$C_{L_o}^2 = \left(\frac{4\alpha}{3\gamma}\right). \qquad (10)$$

The coefficients γ and b are estimated from the hydroelastic data as described shortly. The modal oscillation is assumed sinusoidal and therefore it may be expressed from equation (1) as

$$y_n'' + \eta_T Y'' + y_n = \left[\frac{1/2\rho t^2}{m_s \Omega^2}\right] \left(\frac{\omega_s}{\omega_n}\right) C_L \qquad (11)$$

where we have incorporated the added mass and hydrodynamic damping effects in m_s and in η_T. We have let $\eta_s = \beta/|\omega|$, $\eta_T = \eta_n + \eta_s$ and we have let $p_e(\tau) = qC_L \cos \omega_s \tau$. Equations (9) and (11) may be solved in approximate form by assuming steady state solutions as shown by Hartlen and Currie (1970) or may be solved more exactly on an analog computer. In either case, γ and b remain the undetermined coefficients. An examination of possible solutions of equations (9) and (11) discloses that b affects the frequency bandwidth, $\Delta f/f_s$ of the lock-in region and γ affects the peak so that the maximum amplitude is linearly proportional to γ. Figure 13 shows calculated amplitudes of motion $(Y_n)_{rms}$ for the (3,0) mode of the brass

*Details of the wake survey will be published in the final report of this work.

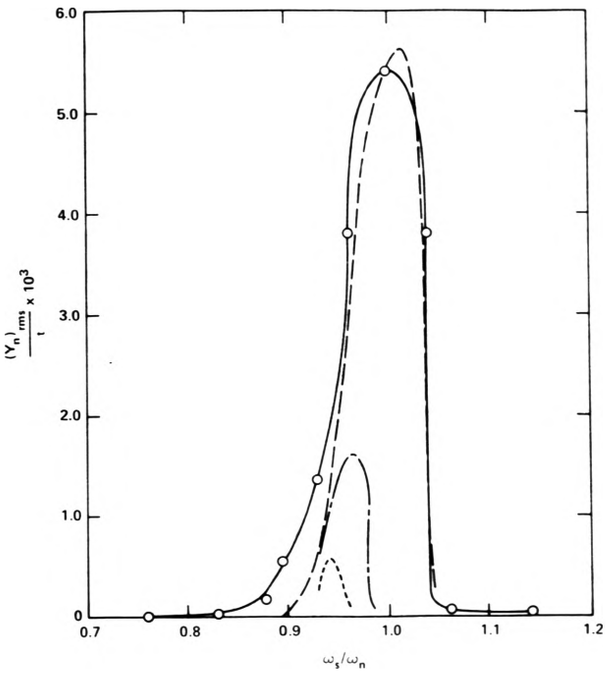

Figure 13 - Modal Displacement Amplitudes for the (2,0) Bending Mode of a Cantilever Stainless Steel Strut. Legend: Measured points -·-; Calculated Values are for η_s=0.0028 (- -), η_s=0.0056 (—-—), and η_s=0.010 (---).

undamped strut as a function of the frequency ratio ω_s/ω_n. The calculation for $\eta_s = 2.8 \times 10^{-3}$ was conducted first and it served to define γ and b by a trial- and -error curve-fit. With the coefficients thus defined, amplitudes were calculated for higher values of damping. It is to be noted that an increase in damping by a factor of two resulted in an estimated reduction in maximum amplitude by a factor of 4. The results of the calculations for the t=0.072 inch edge are shown in Figure 12 as well as additional calculations for t=0.026 inch. The excellent agreement between the measured and calculated damping dependencies lends encouragement to further use of the model. It also indicates that the coefficients γ and b are constant over the modest range of Reynolds numbers covered by the vibration measurements as well as being independent of amplitude.

CLOSURE

The random flow excitation of struts has been analytically predicted using a procedure developed for the estimation of modal response. This technique has been successful for both boundary layer and inflow turbulence excitation. In more recent investigations, the methods have been extended to apply to the linear and non-linear forcing due to vortex street formation.

The relationship has been shown between the linear vortex flow excitation of hydrofoils with the circulatory characteristics of their periodic wakes. The linear excitation occurs with the non-resonant response of lightly damped modes and with the resonant response of modes with structural loss factors which exceed 3×10^{-2}. Comparisons of measurements of flow-induced acceleration on vibrating hydrofoils and of the aerodynamic pressure fields induced on rigid struts by their wakes have formed the basis of this comparison. In these cases of linear excitation of hydrofoils by vortex streets, a reliable prediction method for determining response to known oscillatory pressures is shown. Empirical data for these pressures or a semi-empirical relationship between the pressures and the wake statistics appear to be more reliable than purely theoretical estimates in determining excitation functions.

In the case of moving edges, it appears that non-linear empirical models such as that proposed by Hartlen and Currie (1970) will become increasingly important. An experiment which is directed at giving physical significance to the coefficients of the model is currently underway. The approach is to determine the influence of trailing edge motion on the lift coefficient in so far as it alters the strength of shed vortices and the phase between the motion of the surface of flow-separation and the resulting vortex at its formation point. Preliminary data shows that the motion increases the levels of the pressures as well as the strengths and spanwise coherence of the shed vortices. Also, when $f/f_s \approx 1$ the pressures are in phase with the velocity of the edge. Thus the effect of the vortices becomes as a negative damping term in equation (1). These effects were observed to become apparent when $y_{rms}/t > 3 \times 10^{-3}$ and they are dependent on Reynolds number.

ACKNOWLEDGMENT

Tha authors appreciate the assistance of L. Maga, E. Howerton, and G. Finkelstein in obtaining the experimental data. This work was sponsored by the David W. Taylor Naval Ship Research and Development Center In-House Independent Research Program, and by the Naval Sea Systems Command, Code 037.

REFERENCES

1. Bearman, P.W., (1965) "Investigation of the Flow Behind a Two-Dimensional Model with a Blunt Trailing Edge and Fitted with Splitter Plates" J. Fluid Mech. 21, p. 241-255
2. Bearman, P.W. (1967) "On Vortex Street Wakes" J. Fluid Mech. 28 p. 625-641
3. Blake, W.K., (1975) "A Statistical Description of Pressure and Velocity Fields at Trailing Edges of Flat Struts," NSRDC Report 4241, Dec. 1975
4. Blake, W.K. and Maga, L.J. (1973) "The Vibratory Dynamics of Flow-Excited Struts in Water" NSRDC Report 4087, Dec. 1973
5. Blake, W.K. and Maga, L.J. (1975a) "On the Flow-Excited Vibrations of Cantilever Struts in Water, I - Flow-Induced Damping and Vibration," J. Acoust. Soc. Am. 57, p. 610-625
6. Blake, W.K. and Maga, L.J. (1975b) "On the Flow-Excited Vibrations of Cantilever Struts in Water, II - Surface Pressure Fluctuations and Analytical Predictions," J. Acoust. Soc. Am. 57, p. 1448-1464
7. Fage, A. and Johanson, F.C. (1927) "On the Flow of Air Behind an Inclined Flat Plate of Infinite Span" Proc. Roy. Soc. A116, p. 170-197
8. Griffin, O.M., Skop, R.A. and Koopman, G.H. (1973) "The Vortex-Excited Resonant Vibrations of Circular Cylinders," J. Sound & Vib. 31, p. 235-249
9. Hartlen, R.T. and Currie, I.G. (Oct 1970) "Lift-Oscillator Model of Vortex Induced Vibration", J. Am. Soc. Civil Eng. J. Engineering Mech. Div. No. EM 5, p. 577-591
10. Mugridge, B.D. (1970) "The Generation and Radiation of Acoustic Energy by the Blades of a Sub-Sonic Axial Flow Fan Due to Unsteady Flow Interaction" Univ. Southampton, Ph.D. thesis.
11. Ross, D., Ungar, E.E., Kerwin, E.M., Jr. (1959) "Damping of Plate Flexural Vibrations by Means of Viscoelastic Saminar" Paper in "Structural Damping," ASME Colloquium on Structural Damping, J.E. Ruzicka, Ed.
12. Schaefer, J.W. and Eskinazi, S (1959) "An Analysis of the Vortex Street Generated in a Viscous Fluid" J. Fluid Mech. 6, p. 241-260
13. Skop, R.A. and Griffin, O.M. (1973) "A Model for the Vortex-Excited Resonant Response of Bluff Cylinders," J. Sound and Vib. 27, p. 225-233

DISCUSSION

R. Brown, Naval Underwater Systems Center: Have you noticed any coupling between shed vortices and the leading edge, laminar portion of the boundary layer? This has been reported to cause intense, coherent components in strut vibration.

Blake: The formation of disturbances, especially well-correlated ones, at trailing edges could cause some oscillation of the potential fluid flow. This motion could conceivably be coupled to the leading-edge flow and thus cause a "wandering" of the stagnation point there. In our wind tunnel measurements of the fluctuating pressures on struts, we have found no evidence of this.

Bob Ash, Old Dominion University: In your measurements of your structurally damped experiments how did you compensate for the air damping that occurs even without flow? Did you take that into consideration?

Blake: Yes, we considered these losses. The cantilever beams were clamped in a 200 lb. block of stainless steel. In air, damping of the beams without damping treatment was controlled by losses in the clamp. In stagnant water, the damping of the untreated beams (Figure 7) was controlled by the losses in the clamp with a small contribution at low frequencies due to viscous losses in water. (See also Blake, W.K., "On Damping of Transverse Motion of Free-Free Beams in Dense, Stagnant Fluids," Shock and Vibration Bulletin No. 42, Jan. 1972.